

TEXTILE BELT SPLICE ANALYSIS USING FINITE ELEMENT METHOD

P. Heitzmann¹, A. Wakatsuki², L. Overmeyer¹

¹Institute of Transport and Automation Technology, Leibniz Universität

²Fenner Dunlop – Engineered Conveyor Solutions

1. INTRODUCTION

When considering the investment costs of a conveyor system, it must be remembered that the conveyor belt has a decisive role when it comes to the design of the system. The individual belt segments are spliced at the system to form an endless belt. In the spliced sections, the tension force of the belt is transferred via the skim rubber from one belt end to the other, which makes splices the weakest points of a conveyor belt. Besides system requirements and economic reasons, the tension members are made of steel cords or textile layers depending on nominal strength requirements¹. Textile belts can consist of multiple fabric plies. The number of layers and the tensile strength of the fabric define the splice layout. In most cases, a finger splice design is used for single-ply belts, and multi-ply belts are spliced using a step design (Figure 1). The achievable splice strength is directly related to the design. In a step splice of n fabric layers, the tension force is carried by $n-1$ layers. Therefore, for a three-ply belt, the maximum splice strength is 66%. The theoretical achievable strength of a finger splice is approximately 90%, which is defined by the total cross section of the fingers^{2, 3, 4}.

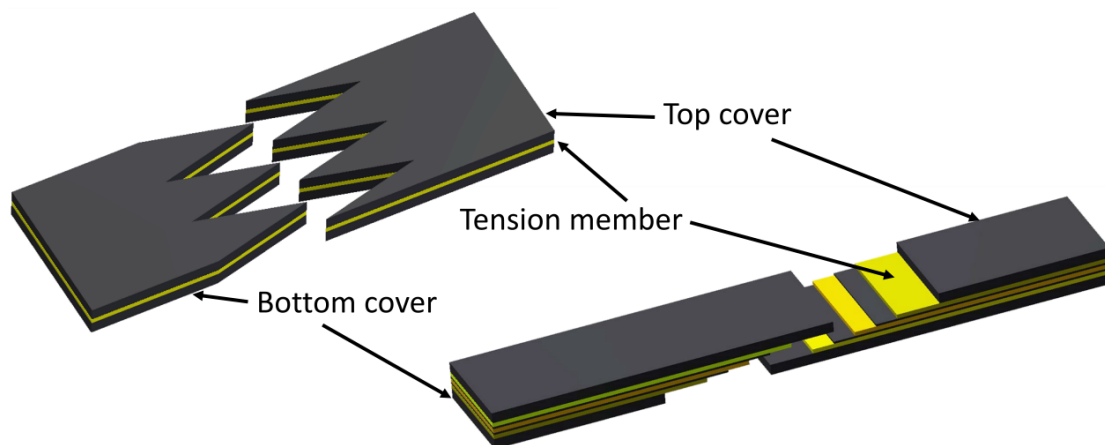


Figure 1. Textile belt splice: finger splice (left) and step splice (right).

The experimental testing of a conveyor belt splice is standardised in DIN 22110-3, which provides the time fatigue curve of a splice⁵. This testing procedure is very time-consuming and cost-intensive^{6, 7}. During the test, it is possible to measure the overall tension of the test belt sample, but not the local tension in the tension member or the shear stress in the skim rubber. The use of the finite element analysis provides an opportunity to determine stress and strain in the individual components of a belt splice. With FEA, the stress and tension curve can be simulated^{8,9}. Therefore, the use of FEA is an effective tool to optimise the belt splice design. The required information to set up an FEA-model of a textile belt splice is shown in

Figure 2. It is divided into two main sections. First, there is the geometric data, which is related to the belt and splice design. The second section is the definition of the material properties, which are related to the individual components and the resulting material behaviour. The determination of the required parameters to define the material properties for numerical material models has to be performed via experimental testing.

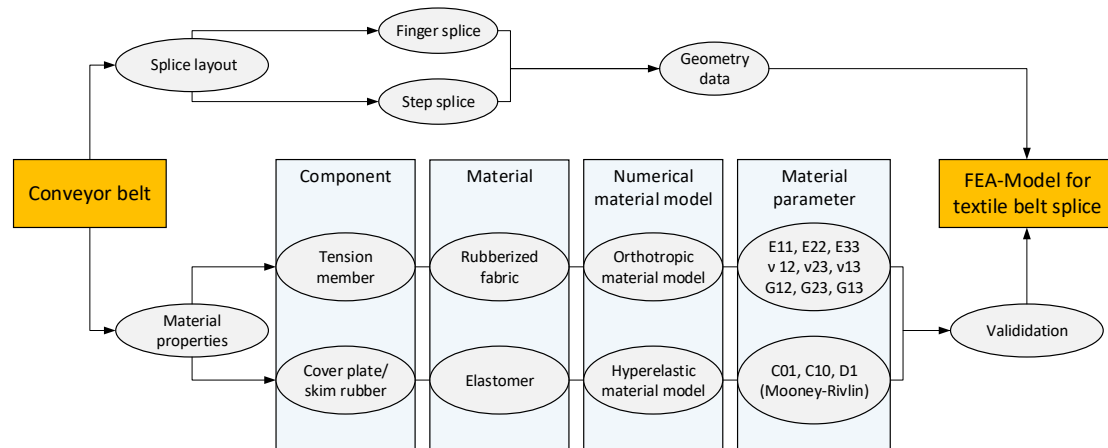


Figure 2. Required data for FEA-model of textile belt splice.

2. NUMERICAL FOUNDATIONS FOR FEA-MODEL

The individual components of a textile belt splice lead to different material behaviour, which can be separated in two sections. On the one hand, there are the components that consist of rubber, cover plates and skim rubber, and on the other hand is the tension member that is a composite material of rubber and fabric. These two material classes need different numerical models to define the material behaviour for the FEA-model. Rubber, which belongs to the material group of elastomers, shows hyperelastic behaviour. Rubberised fabric has orthotropic material properties. Therefore, two different numerical models have to be defined to set up the FEA-model. Hooke's Law

$$\sigma_{ij} = C_{ijkl} \epsilon_{kl} \quad 1$$

specifies the orthotropic elastic behaviour of the belt carcass and shows the proportional relation between stress σ and strain ϵ , with the constant C as material tensor. An orthotropic material behaviour is defined via a material tensor with nine different parameters that define the behaviour for each spatial direction and leads to the following stiffness matrix:

$$C^{-1} = \begin{bmatrix} E_{11} & -\frac{\nu_{12}}{E_{11}} & -\frac{\nu_{13}}{E_{11}} & 0 & 0 & 0 \\ & E_{22} & -\frac{\nu_{23}}{E_{22}} & 0 & 0 & 0 \\ & & E_{33} & 0 & 0 & 0 \\ & & & \frac{1}{G_{12}} & 0 & 0 \\ \text{sym.} & & & & \frac{1}{G_{23}} & 0 \\ & & & & & \frac{1}{G_{13}} \end{bmatrix} \quad 2$$

The material properties are defined by the parameters Young's Modulus E_{11} , E_{22} , E_{33} , Poisson's Ratios ν_{12} , ν_{23} , ν_{13} and Shear Modulus G_{12} , G_{23} , G_{13} . The 1-direction defines

the material properties in running direction of the belt, the 2-direction in transverse direction and the 3-direction in belt thickness direction.

Elastomers show a totally different behaviour compared to the tension member. It is characterised by its hyperelasticity, which can be transferred to the FEA via entropy-elastic numerical material models. One possibility in specifying the numerical models is to use strain energy functions ψ , that are based on strain energy density W and volume change density U :

$$\psi = \psi(I_1, I_2, I_3) = W(I_1, I_2) + U(I_3) \quad 3$$

This can be written with a polynomial approach as:

$$\psi = \sum_{i+j \geq 1}^N C_{i,j} (I_1 - 3)^i (I_2 - 3)^j + \sum_{k=1}^N D_k (I_3 - 1)^k \quad 4$$

Due to the fact that elastomers can be considered as incompressible, the volume change density is negligible. The choice of the numerical model is based on the scope of application. For smaller strains up to 100%, the polynomial approach

$$W = C_{10}(I_1 - 3) + C_{01}(I_2 - 3) \quad 5$$

according to Mooney-Rivlin is valid. The material parameters C_{01} and C_{10} have to be calculated by means of the shear modulus of an elastomer^{10, 11}.

The material parameters to define the stiffness matrix for the tension member and polynomial approach of the rubber components have to be determined by experimental tests¹². This part of the project between Fenner Dunlop and ITA has already been published^{8, 9} and represents the fundamental basis for the following set-up of an FEA-model for textile belt splices.

3. THEORETICAL BEHAVIOUR OF TEXTILE BELT SPLICES

As shown before, textile belts are spliced with two different techniques for permanent belt splices. The various splices also show different performance of force transmission. These different behaviours are shown in the following sections.

3.1. STEP SPLICE

As mentioned, the force transmission is carried out by $n-1$ fabric layers. The transmission can be shown in mathematical terms, with equation 1, as

$$\frac{F_{11}}{A_{tension\ member}} = E_{11} \varepsilon_{11} \quad 6$$

Here, the cross sectional area of tension member $A_{tension\ member}$ and the Young's Modulus E_{11} of the fabric ply are constant. Thus, to transfer the force from one end of the belt to the other, the strain in the fabric layer reduces at one side and increases on the other side. Figure 3 shows this effect³. In principle, it is the same force transmission behaviour as in steel cord splices between two neighbouring cords from different belt ends¹⁴. For a one-step splice, the strain doubles between the layers, because in this area one-ply carries the entire load.

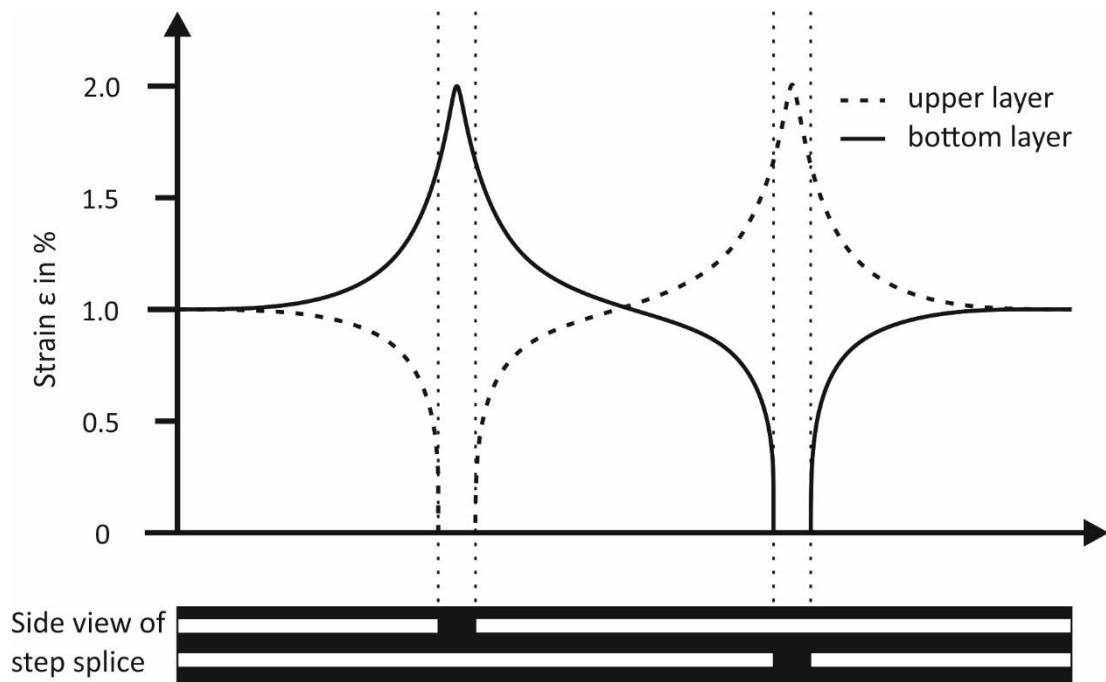


Figure 3. Theoretical strain behaviour of a one-step splice according to Oehmen¹⁴.

3.2 FINGER SPLICE

Finger splices show a different behaviour in force transmission compared to step splices. Considering Equation 6, the transmission depends on the total cross-section of the fingers from one belt end. In contrast to step splices, the cross-section of the tension member is not constant. Depending on the pull-back and finger geometry, the overall cross-section in the splice is reduced by the skim rubber width. This width is specified by pull-back, finger length and finger base, (Figure 4) and can be calculated via

$$\psi = \arctan\left(\frac{\text{Finger length}}{\frac{1}{2}\text{Finger base}}\right) \quad 7$$

and

$$\text{skim rubber width} = 2 * \tan(90 - \psi) * \text{Pullback} \quad 8$$

The overall cross-section of a finger splice is reduced by the skim rubber width multiplied by the number of fingers on one side of the belt. This change (Figure 5) leads to a higher strain in the fingers of a splice compared to the regular belt and can be considered as remaining constant by neglecting some local deviations.

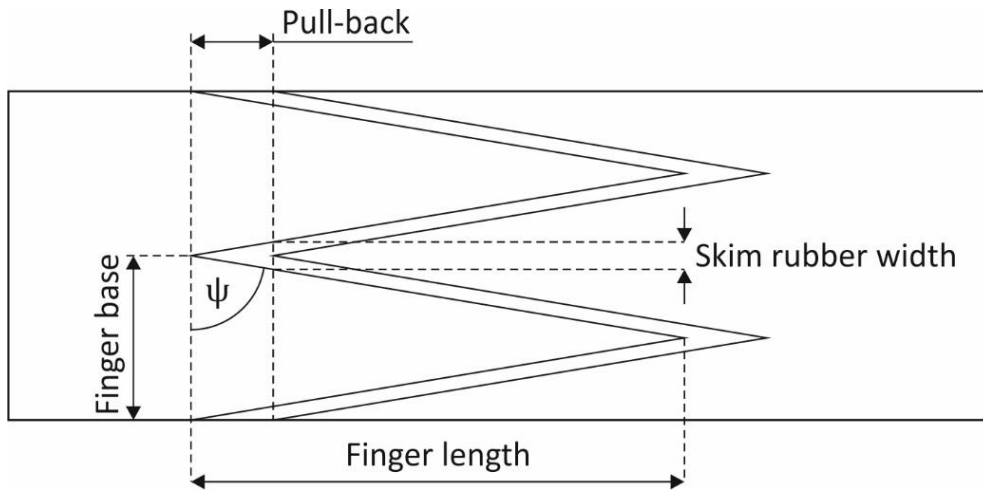


Figure 4. Geometry of a finger splice.

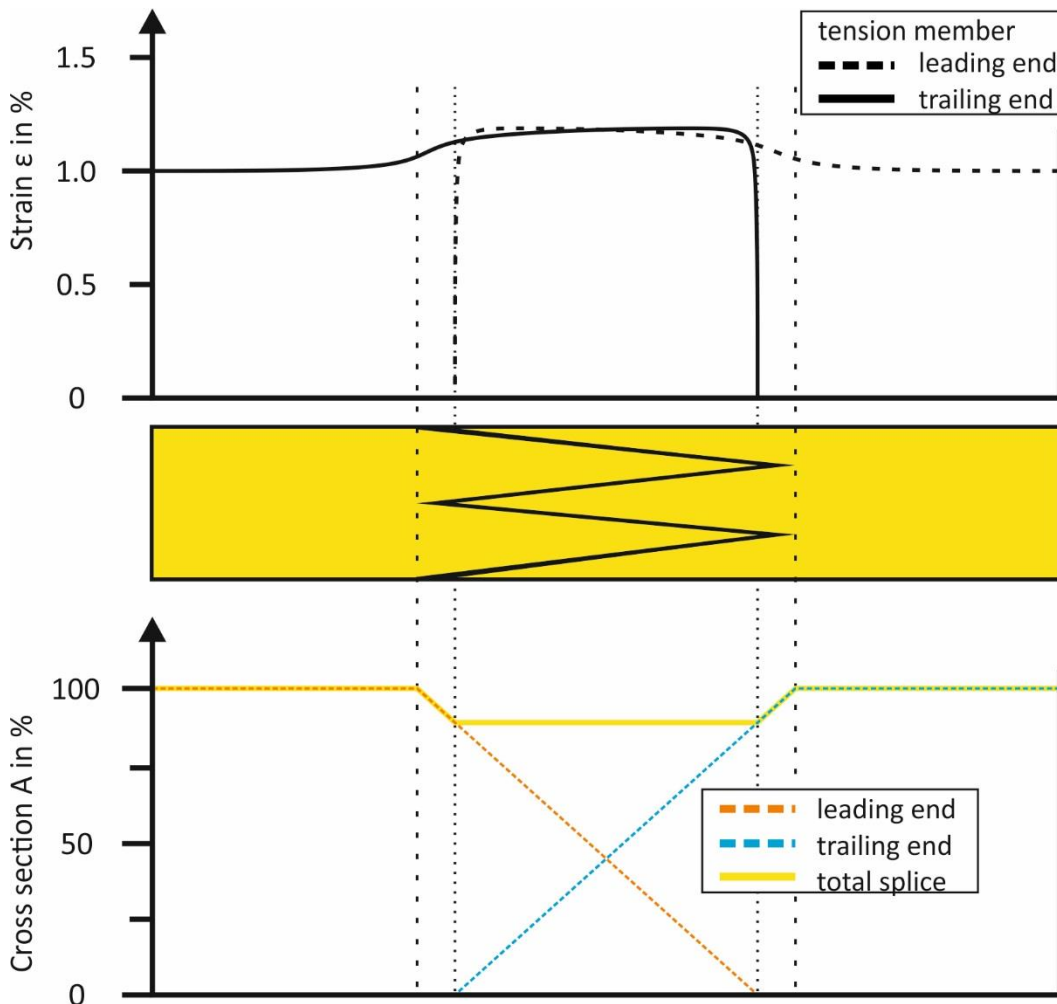


Figure 5. Theoretical strain behaviour of a finger splice and variation of the total cross-section A of the tension members.

These theoretical analyses are essential to understand the behaviour of textile belt splices and serve as a basis to validate the FEA-models that are shown in the upcoming sections.

4. SIMULATION OF TEXTILE BELT SPLICES USING FEA TO PERFORM PARAMETER STUDIES

The general behaviour of textile belt splices, shown in the previous section, is influenced by several geometrical parameters. These parameters are investigated in the following studies, which are constrained by the parameters that can be varied without changing the belt structure. Therefore, the general setup of each FEA-model is explained and checked in terms of its suitability. The general structure of the models is shown in Figure 6. It can be partitioned into three segments, which include the two belt ends (head and tail) and the splice area. As boundary conditions, the model is fixed at the trailing end and a tensile force respectively; a displacement is applied at the leading end. The displacement is set to a resulting belt strain of 3%, according to manufacturer's specifications, where the total elongation of a textile belt is 1.3% to 3.5% at 10% load of the nominal belt strength¹⁵.

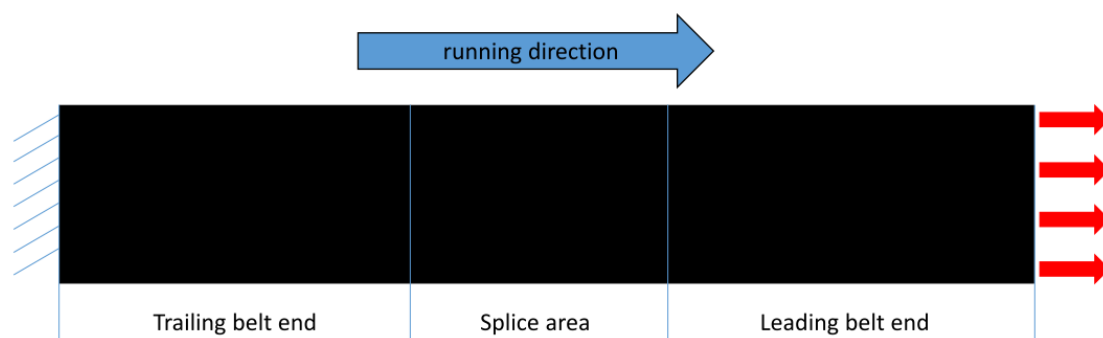


Figure 6. Setup of FEA-model for textile belt splices.

4.1 STEP SPLICE

For step splices, the only modifiable geometrical parameter is the step length. The pull-back of the different belt ends has no influence on the strain in the textile layers. The parameter studies are performed with a two-ply belt. The simulated strain behaviour of the FE-model is shown in Figure 7. The typical influence of boundary conditions can be seen at both belt ends, but can also be neglected because of the constant strain between these effects and the splice area. The green curves show the strain curve of the trailing end while the strain in the leading end is marked in blue. These results match the theoretical analysis of a one-step splice shown in Figure 3. The strain of the remaining ply in the area between two belt ends increases by 100 % (from 1.8% to 3.6%).

The force transmission behaviour in the tension members can be seen in the strain reduction of the trailing end and the opposing increasing of strain in the leading end. These results show the potential use of the FEA-model for further parameter studies on textile belt splices. In one of these studies, the step splice varies from 400 mm to 550 mm. The applied displacement at the leading end of the belt is equivalent to a total elongation of 3% of the total belt length. The result of the parameter studies is shown in Figure 8. For a better overview, only the strain of the minimum step length of 400 mm (orange) and the maximum step length of 550 mm (grey) is charted in the graph. There is no recognizable change in strain behaviour. The variation of the step length only creates an area in the splice where no force transmission occurs with a

constant strain that is equivalent to the strain outside the splice. Therefore, the increase of the step length has no effect on the behaviour of the splice.

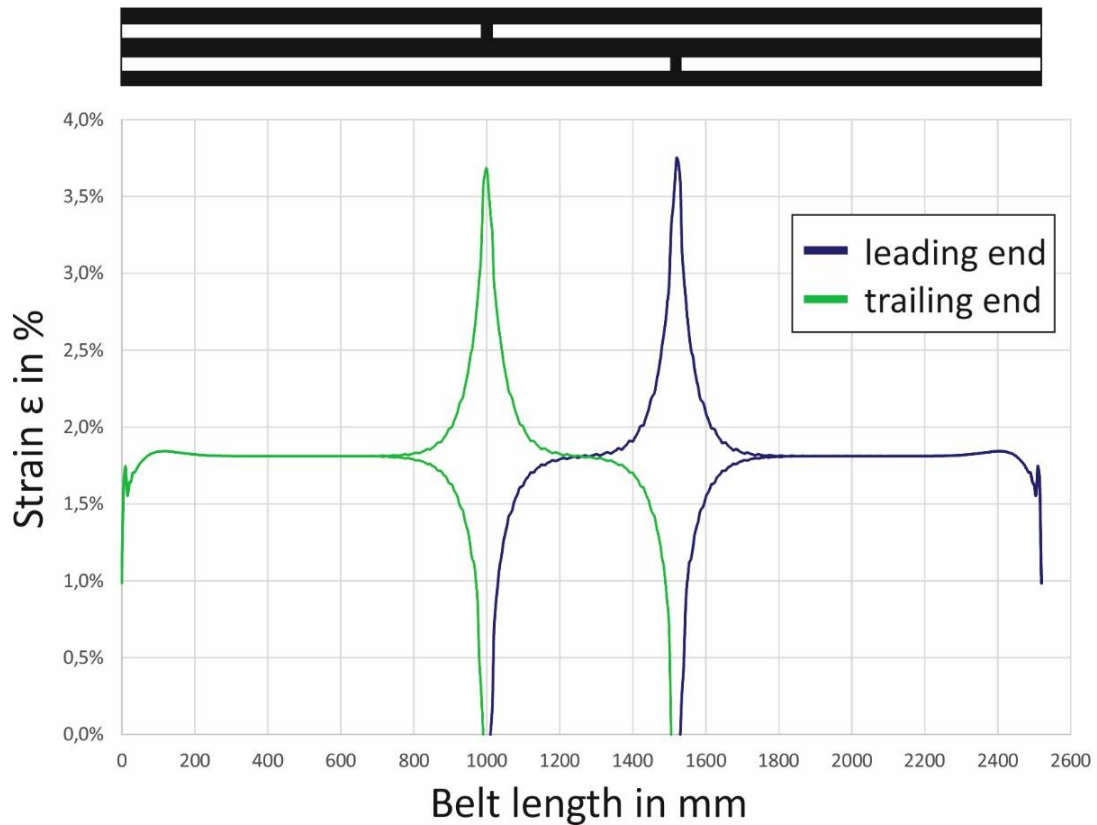


Figure 7. Simulated strain behaviour of FEA-model for a one-step splice.

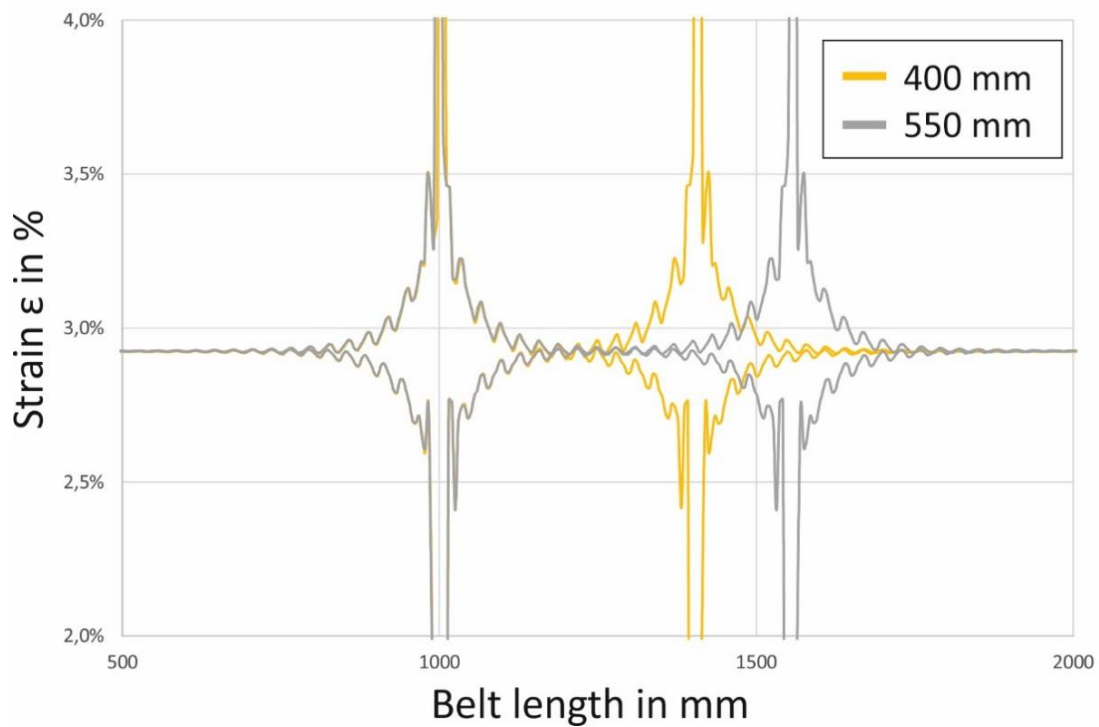


Figure 8. Results of parameter studies on varying step splice length of a one-step splice.

4.2 FINGER SPLICE

The geometry of a finger splice is defined by the finger length, finger base and pull-back between the belt ends. These are the most important parameters which can be varied without changing the belt structure. Figure 9 shows the results of the FEA-model which is used in the following parameter studies. It shows the strain distribution for an applied displacement that corresponds to a strain of 3% for the entire model. The strain behaviour matches the theoretical approach from section 3.2. The model fulfils the requirement of constant strain in the belt. Thus, the boundary effects due to clamping and displacement areas can be neglected. The result shows constant strain in all three segments. Less strain appears in head end and trailing end than in the splice itself. The strain behaviour is also shown in Figure 10. Due to the symmetry of the splice (compare Figure 9), the graph shows only the strain of one finger from each side at the neutral axis in the middle of the fingers.

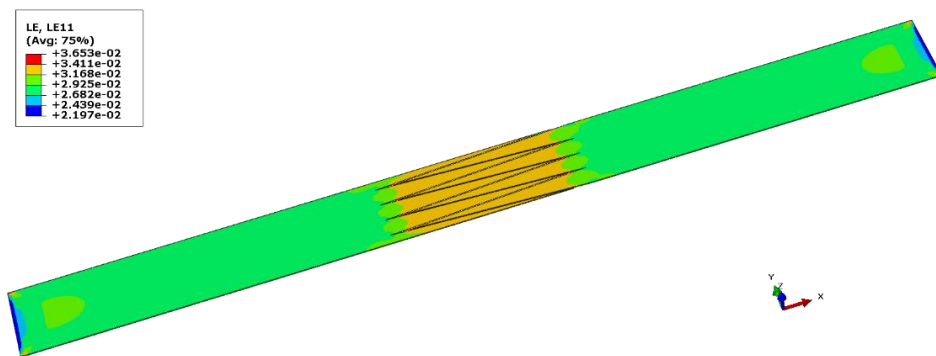


Figure 9. Simulated strain in finger splices using FEA.

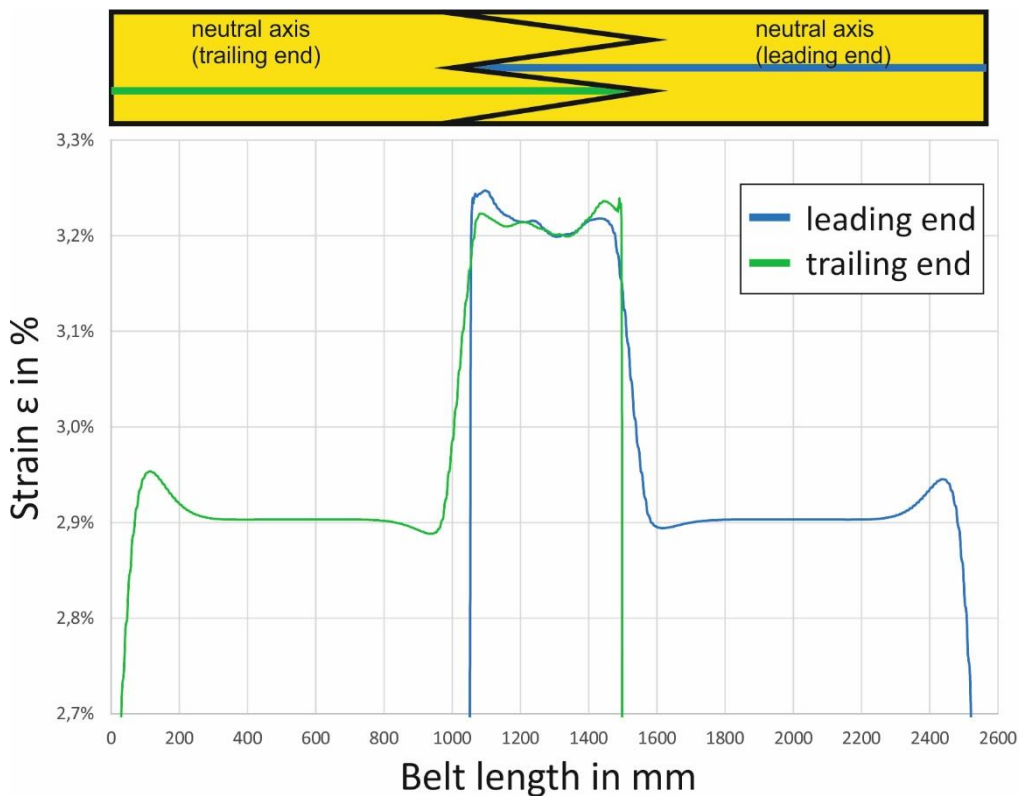


Figure 10. Simulated strain in finger splices.

Neglecting the boundary effects that are caused by the clamping of the model, the apparent strain in the belt is 2.9%. The strain in the splice, considering Equation 7 and the reduced total cross-section of the tension member in the splice should be 3.2%. The mean value of the simulation is 3.19%, which represents a divergence of 0.003 from the predicted value. This ensures a sufficient accuracy of the FEA-model. It has to be mentioned that the occurring strain has some local variations. The results show for example, slightly higher strain at the fingertips. These local effects are not considered in the following studies.

The first geometrical parameter to be investigated is the finger length. For this study, the finger base (50 mm) and the pull-back (50 mm) are constant. The finger length is varied from 400 to 650 mm and the total cross-section of the tension member in the splice A_{splice} is calculated. Based on this value, the strain in the splice $\epsilon_{splice,predicted}$ is determined in relation to the strain in the regular belt ϵ_{belt} , which is taken from the simulation. To verify the theoretical hypothesis of the behaviour for finger splices, the divergence of predicted strain $\epsilon_{splice,predicted}$ and simulated strain $\epsilon_{splice,simulation}$ is calculated. The results of the subsequent parameter studies are shown in Table 1.

Finger length FL in mm	Cross section A_{splice} (in % of A_{belt})	Strain ϵ_{belt} in %	Strain $\epsilon_{splice,predicted}$	Strain $\epsilon_{splice,simulation}$	Divergence in %
400	87.5	2.9	3.31	3.28	0.9
450	88.9	2.9	3.26	3.25	0.3
500	90.0	2.9	3.22	3.21	0.3
550	90.9	2.9	3.19	3.18	0.3
600	91.7	2.9	3.16	3.16	0.0
650	92.3	2.9	3.14	3.14	0.0

Table 1. Parameter studies on variation of finger length.

The variation of the finger length shows that, if the length is increased, the cross-section increases as well. This leads to lower strain inside the splice (Figure 11). With increasing finger length, the local variations are reduced, which leads to a more constant strain behaviour in the splice. Using a smaller finger base basically has the same effect as increasing the finger length. It leads to a lower ratio of finger base to finger length.

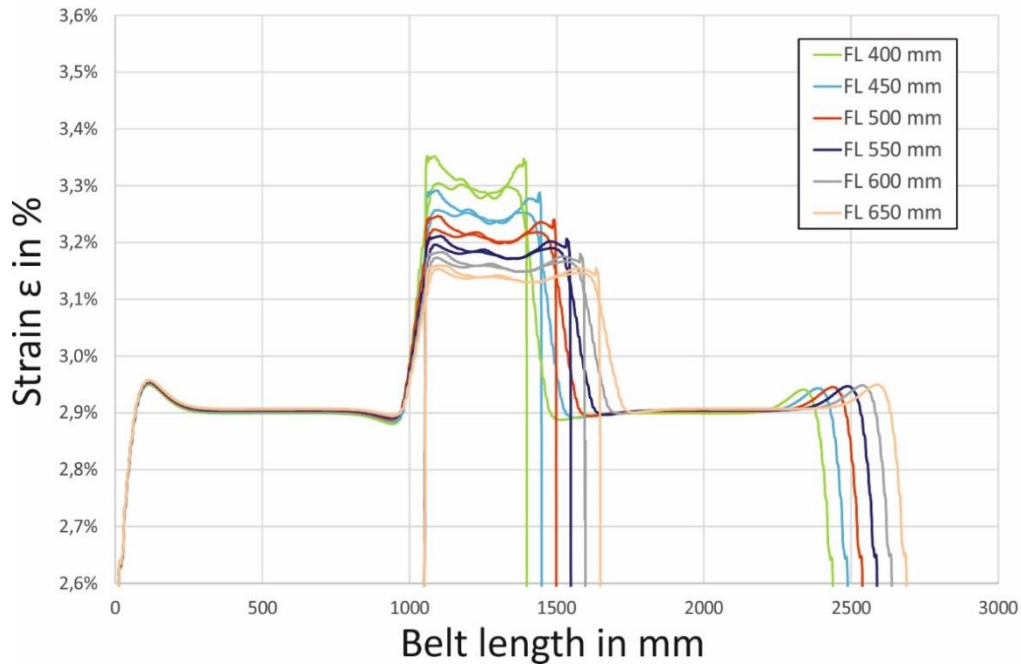


Figure 11. Parameter studies on variation of finger length.

The total cross-section of the tension member in a splice is also defined by the pull-back. The influence is investigated in the following parameter studies. Here, the finger length (500 mm) and the finger base (50 mm) are constant. Table 2 shows the effect on the splice behaviour if the pull-back is varied. A larger pull-back results in a smaller cross-section A_{splice} . This value and the strain in the belt ϵ_{belt} leads to the predicted strain in splice $\epsilon_{splice, predicted}$, which can be compared with the simulated strain in the splice $\epsilon_{splice, simulation}$. Figure 12 shows the graph relevant to the calculated values of Table 2.

Pull-back PB in mm	Cross section A_{splice} (in % of A_{belt})	Strain ϵ_{belt} in %	Strain $\epsilon_{splice, predicted}$	Strain $\epsilon_{splice, simulation}$	Divergence in %
50	90.0	2.90	3.22	3.21	0.3
60	88.0	2.89	3.28	3.26	0.6
70	86.0	2.88	3.35	3.32	0.9
80	84.0	2.86	3.41	3.39	0.6
90	82.0	2.85	3.48	3.45	0.9
100	80.0	2.83	3.54	3.51	0.8

Table 2. Parameter studies on variation of pull-back.

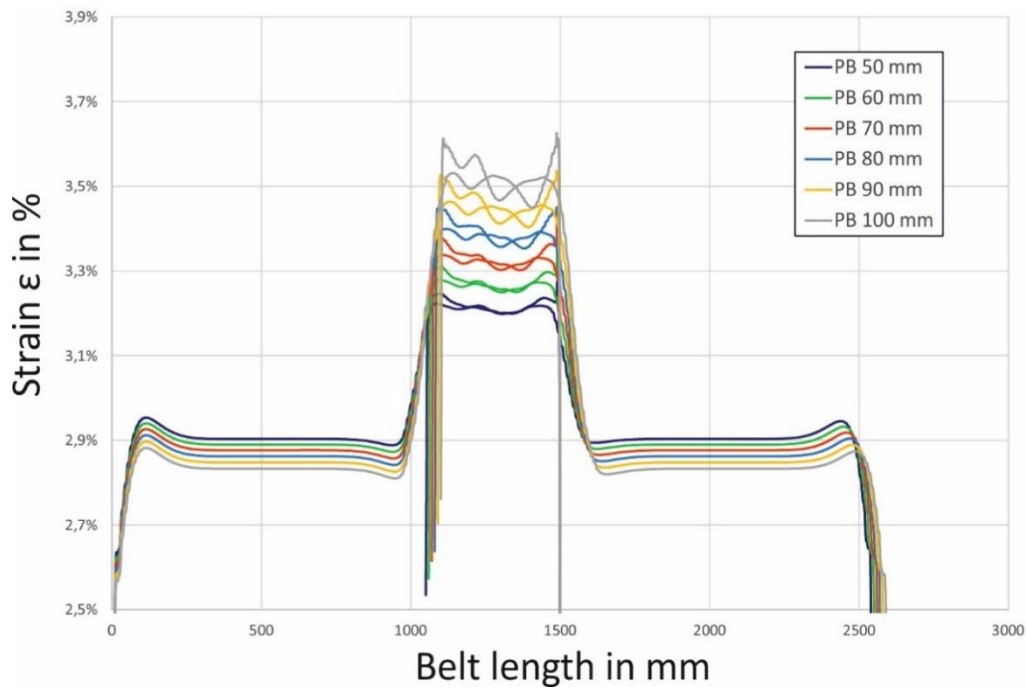


Figure 12. Parameter studies on variation of pull-back.

The results show that a bigger pull-back leads to higher strain in the splice. Another effect of an increasing pull-back is a lower stiffness of the splice, which can be assumed due to smaller strain outside the splice.

The performed parameter studies using the finite element method show the effect of variation of the finger length and the pull-back. The increase of a finger length and a smaller pull-back leads to smaller strain of the tension member inside a finger splice (Figure 13).

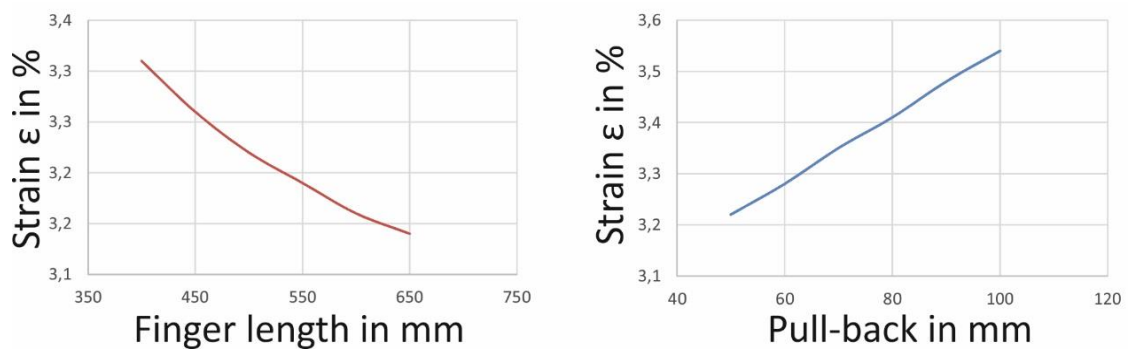


Figure 13. Strain behaviour of a finger splice in relation to a varying finger length (left) and pull-back (right).

The created FEA-model for finger splices is applied in the upcoming case study to show the application possibilities of using FEA for finger splices.

5. CONCLUSIONS

The development of FEA-models for textile belt splices based on numerical and theoretical foundations has been presented. The case study illustrated demonstrates the potential to use FEA to analyse and optimise textile belt splices.

Furthermore, the FEA-models were used to perform parameter studies to determine the general strain behaviour depending on geometrical parameters that are not defined by the belt structure. For step splices, the only modifiable geometrical parameter is the step length. The studies show that there is no noticeable influence on the strain behaviour if the step length is increased. This effect and the fact that the strength of a step splice is defined by $n-1$ plies, will engender further investigations focusing on step splices using intermediate plies.

There are more geometrical possibilities that influence the behaviour of a finger splice other than a step splice. The geometry of the finger is defined by the ratio of finger length and finger width at the base, and the pull-back between both belt ends. The parameter studies prove the theoretical approach.

By neglecting local deviations, the strain in a finger splice can be assumed to be constant. The modification of the finger length shows that an increased length leads to less strain in the splice, whereas an enlarged pull-back causes a higher strain inside the splice. Both effects are coupled with the change of the skim rubber width. The strain inside a finger splice is higher if the skim rubber width is increased. Optionally, additional breakers are used inside a finger splice. The next step is to implement a breaker in the FEA-model for finger splices to investigate if there is any resulting increase in strength.

The FEA-models were used to perform qualitative research on the general behaviour of textile belt splices. They are able to analyse the stress strain behaviour that occurs inside a splice. To predict a failure of the splice, additional material tests are necessary to define a quantitative material failure.

In conclusion, FEA-models can be used for determination of optimum splice dimensional parameters. This will save time and cost, because experimental investigations are reduced and only needed for certification process in ideal circumstances.

REFERENCES

- 1 Ziller, T. and Hartlieb, P. (2010). Fördergurte in der Praxis - Know How and Know Why. NILOS GmbH & Co. KG. VGE Verlag. Deutschland. ISBN 978-3-86797-105-8
- 2 DIN 22101: Stetigförderer – Gurtförderer für Schüttgüter – Grundlagen für die Berechnung. Normausschuss Bergbau (FABERG) im DIN und Normenausschuss Kautschuktechnik (FAKAU) im DIN. Beuth Verlag GmbH. Berlin, Germany. 2011
- 3 CEMA. (2005). Belt Conveyors for Bulk Materials – sixth edition. USA. ISBN 1-89117-59-3
- 4 DIN 22102-3: Textil-Fördergurte für Schüttgüter – Teil 3: Nichtlösbare Fördergurtverbindungen. Normausschuss Bergbau (FABERG) im DIN und Normenausschuss Kautschuktechnik (FAKAU) im DIN. Beuth Verlag GmbH. Berlin, Germany. 2014

- 5 DIN 22110-3: Prüfverfahren für Fördergurtverbindungen – Teil 3: Ermittlung der Zeitfestigkeit für Fördergurtverbindungen (Dynamisches Prüfverfahren). Normausschuss Bergbau (FABERG) im DIN und Normenausschuss Kautschuktechnik (FAKAU) im DIN. Beuth Verlag GmbH. Berlin, Germany. 2015
- 6 Overmeyer, L.; Froböse, T. and Radosavac, M. (2012). Trends and experiences of testing the fatigue strength of more than 1000 conveyor belt splices. Proceedings of XX international Conference on Material Handling, Constructions and Logistics. Belgrad, Serbia. MHCL
- 7 Hötte, D.; Lotz, C.; Froböse, T. and Overmeyer, L. (2015). Trends in der frühzeitigen Schadensanalyse von Fördergurtverbindungen während der Umlaufprüfung. 20. Fachtagung Schüttgutförderertechnik. Magdeburg, Germany.
- 8 Froböse, T.; Heitzmann, P.; Wakatsuki, A. and Overmeyer, L. (2014). Entwicklung eines FE-Modells zur Optimierung von Stahlseil-Fördergurtverbindungen – Development of a FE-model to optimize steel cord conveyor belt splices. Logistics Journal. WGTL. ISSN 2192-9084
- 9 Heitzmann, P.; Froböse, T.; Wakatsuki, A. and Overmeyer, L. (2016). Optimierung von Textil-Fördergurtverbindungen mittels Finite Elemente Methode (FEM) – Optimization of textile conveyor belt splices using Finite Element Method (FEM). Logistics Journal. WGTL. ISSN 2192-9084
- 10 Wrigger, P. (2008). Nonlinear Finite Element Methods. Springer Verlag. Berlin Heidelberg, Germany. ISBN 978-3-540-71000-4
- 11 Strommel, Stojek and Korte (2011). FEM zur Berechnung von Kunststoff- und Elastomerbauteilen. Hanser Verlag, München, Germany.
- 12 Bergström, J. (2015). Mechanics of Solid Polymers – Theory and Computational Modeling. ELSEVIER Science Publishing Co Inc. ISBN 978-0-323-31150-2
- 13 Dora, H. U. and Oehmen, K. H. (1983). Zur Beanspruchung mehrlagiger Textilfördergurte – Stresses and strains in conveyor belts with multiple textile plies. Braunkohle 36 – No. 3 page 65-74.
- 14 Oehmen, K. H. (1977). Zur Berechnung des Kraftflusses in Stahlseilgurtverbindungen – For calculating the force flux in steel rope belt connections. Braunkohle 29 – No. 7 page 268-278
- 15 Jungk, A. (2013). Fördergurte – Berechnungen. Continental AG, Hannover

ABOUT THE AUTHORS



DIPL.-ING. PATRICK HEITZMANN

Research Assistant at the Institute of Transport and Automation Technology of Leibniz Universität Hannover, Germany.

Between 2004 and 2013, he studied mechanical engineering at Leibniz Universität Hannover. In 2010, he was at the Center for Intelligent Systems and Structures (CIMSS) at Virginia Tech, USA as a visiting scholar. Since 2013 he works at the Institute of Transport and Automation Technology of Leibniz Universität Hannover as a research assistant.

PATRICK HEITZMANN

Leibniz University Hannover, Institute of Transport and Automation Technology, An der Universität 2, 30823 Garbsen, Germany

Phone: +49 511 762-18173, Fax: +49 511 762-4007,

E-Mail: patrick.heitzmann@ita.uni-hannover.de



Prof. Dr.-Ing. Ludger Overmeyer

Head of the Institute of Transport and Automation Technology of Leibniz Universität Hannover.

Between 1984 and 1991, he studied electrical engineering at the University of Hannover. In 1996 he finished his doctorate in mechanical engineering at the University of Hannover. From 1997 to 2001 he worked as project manager, division manager and head of research and development at Mühlbauer AG. Since 2001 Ludger Overmeyer is Professor at the Institute of Transport and Automation Technology of Leibniz Universität Hannover.

Ludger Overmeyer

E-Mail: ludger.overmeyer@ita.uni-hannover.de

AKIKO WAKATSUKI

Manager, Conveyor belt application and technical support

Fenner Dunlop – Engineered Conveyor Solutions, 1000 Omega Drive, Suite 1400, Pittsburgh, PA 15205, USA

E-Mail: akiko.wakatsuki@fennerdunlop.com